

# Surfactant-assisted hydrothermal synthesis of chains self-assembled by cobalt microspheres

Y.J. Zhang<sup>\*</sup>, S. Ma, D. Li, Z.H. Wang, Z.D. Zhang

*Shenyang National Laboratory for Materials Science, Institute of Metal Research, and International Centre for Materials Physics, Chinese Academy of Sciences, Shenyang 110016, PR China*

Received 25 December 2006; received in revised form 28 September 2007; accepted 16 November 2007

Available online 22 November 2007

## Abstract

Magnetic cobalt chains, self-assembled by microspheres of hexagonal-phase cobalt, have been synthesized at 100 °C via a hydrothermal reduction route in the presence of cobalt chloride, the surfactant sodium dodecylsulfate (SDS) (or cetyltrimethylammonium bromide CTAB) and the complex reagent sodium tartrate. As-synthesized, the chains are 100–300 μm in length and the cobalt microspheres, which consist of nanosheets with an average thickness of about 60 nm, are 5–10 μm in diameter. The magnetic hysteresis loops at 5 K and 300 K of the chains of microspheres show ferromagnetic characteristics. The morphologies of the microspheres can be controlled by adjusting the concentrations of the surfactant and the complex reagent and also the reaction temperature.

© 2007 Elsevier Ltd. All rights reserved.

*Keywords:* A. Magnetic materials; B. Chemical synthesis; D. Magnetic properties

## 1. Introduction

It is generally believed that the properties of nanomaterials sensitively depend on their size, shape and dimensionality [1]. Recently, considerable attention has been paid to the synthesis of magnetic nanomaterials because of their unique properties and potential application in high-density data storage, medical diagnosis and catalysts [2–4]. However, most of the isolated magnetic nanoparticles with sizes below a critical value (diameter <10 nm for Co) are superparamagnetic at room temperature and thus cannot be used in many fields [5,6]. Although the high-yield synthesis of mono-dispersed magnetic nanoparticles has been achieved, it is still a challenge to control simultaneously their shape, surface structure, and anisotropy. Therefore, great effects have been focused on the fabrication of magnetic nanomaterials with various nanostructures [7–11].

In particular, cobalt is one of the most important ferromagnetic metals. There exist three cobalt phases with different crystallographic structures, namely, the hexagonal (hcp) phase, the face-centered cubic (fcc) phase and the epsilon phase. Generally, the hcp Co phase with a high coercivity is of interest in the field of permanent magnets, while the fcc Co phase with a low coercivity can be used as soft-magnetic materials [12]. Cobalt with different nanostructures can be synthesized in a controlled fashion by means of various physical and chemical methods [13–23],

<sup>\*</sup> Corresponding author.

*E-mail address:* [yjzhang@imr.ac.cn](mailto:yjzhang@imr.ac.cn) (Y.J. Zhang).

among which the chemical-solution-phase method is simple and inexpensive for large-scale preparation. Different reaction conditions and surfactants usually result in various morphologies. Xie et al. [24–25] synthesized cobalt nanobelts and nanowires with a complex reagent and a surfactant under mild hydrothermal conditions. Hou et al. [26] obtained mono-dispersed cobalt spheres consisting of nanoplates using sodium tartrate as complex reagent and sodium dodecyl benzenesulfonate (SDBS) as surfactant. Chain-like cobalt assemblies are important members of 1D structures because they provide a direct bridge between nanometer scale objects to macroscale world [27]. However, chain-like cobalt assemblies have received much less attention. Here, we report a hydrothermal reduction route for fabricating self-assembled hcp-cobalt chains constructed by cobalt microspheres consisting of nanosheets with an average thickness of about 60 nm, by using sodium dodecylsulfate (SDS) or cetyltrimethylammonium bromide (CTAB) as surfactant. In addition, the influence of the reaction conditions on the morphologies of the cobalt microspheres is studied in detail.

## 2. Experimental

All reagents were of analytical grade, purchased from Shenyang Chemical Reagent Company and used without further purification. In a typical experiment, 0.192 g (0.667 mmol) SDS was first dissolved in 35 ml distilled water, then 0.476 g (2 mmol)  $\text{CoCl}_2 \cdot 6\text{H}_2\text{O}$ , 6.9 g (30 mmol)  $\text{Na}_2\text{C}_4\text{H}_4\text{O}_6$  and 1.408 g (16 mmol)  $\text{NaH}_2\text{PO}_2$  were added to the solution. Subsequently, 5 ml NaOH (16 M) solution was put into the above solution under constant magnetic stirring. The mixture was stirred for 30 min and then transferred into a 50 ml Teflon-lined autoclave. After the autoclave was maintained at 100 °C for 10 h, it was rapidly cooled to room temperature by means of water. After having been collected at the bottom of the Teflon-cup, the grey precipitation was first washed with distilled water, then with anhydrous ethanol for several times to remove impurities and finally dried in a vacuum oven at room temperature for 12 h.

The phases in as-prepared products were identified by means of a Rigaku D/max 2500pc X-ray diffractometer (XRD) with Cu K $\alpha$  radiation. The size, morphology and composition of the products were investigated in a Shimadzu SSX-550 scanning electron microscope (SEM) with X-ray energy-dispersive spectroscopy (EDS). X-ray photoelectron spectroscopy (XPS) measurements were performed on an ESCALAB-250 to characterize the valence of cobalt atoms at the surface of the microspheres. Magnetic hysteresis loops were measured in a superconducting quantum interference device (SQUID) magnetometer at fields up to 20 kOe. After cooling the sample from 295 K to 5 K without an applied magnetic field, the zero-field-cooled (ZFC) magnetization was measured from 5 K to 295 K and then the field-cooled (FC) magnetization from 295 K to 5 K, both at an applied magnetic field of 50 Oe.

## 3. Results and discussion

A typical XRD pattern of the sample obtained by the hydrothermal treatment at 100 °C for 10 h is shown in Fig. 1a. All XRD peaks can be indexed as Co with hexagonal structure, consistent with the standard card JCPDS card No. 05-0727 (space group  $P6_3/mmc$ ;  $a = 2.503 \text{ \AA}$ ;  $c = 4.060 \text{ \AA}$ ). No obvious peaks resulted from impurities such as CoO or  $\text{Co}_3\text{O}_4$  are observed, indicating that hexagonal (hcp) phase cobalt is the main product in the sample. The EDS analysis also confirms that the main phase of is pure Co (as shown in Fig. 1b). Only small amounts of oxygen (2.76 wt%) and phosphorus (0.91 wt%) are detected, which indicates the existence of cobalt oxides and some absorbates on the surface. The existence of CoO on the surface of the cobalt microspheres has been established on the basis of the binding energies of satellite peaks at 789.1 eV and 781.2 eV of  $\text{CoO}2p_{3/2}$  and  $\text{CoO}2p_{1/2}$ , respectively, found in the XPS spectrum (Fig. 1c) [28]. Another binding-energy peak at 778.5 eV [29] of  $\text{Co}2p_{3/2}$  indicates that the surface of the cobalt microspheres is oxidized only partially.

The size and morphology of the sample were examined by SEM. A typical low-magnification SEM image (Fig. 2a) reveals that the products are chains composed of Co microspheres. The chains are about several tens of micrometers in length. The average diameter of the microspheres ranges from 5  $\mu\text{m}$  to 10  $\mu\text{m}$ . Fig. 2b represents a typical SEM image of the microspheres with high magnification. It can be clearly seen that the surfaces of the microspheres are not smooth. They consist of well-crystallized nanosheets with an average thickness of about 60 nm, as estimated from the standing nanosheets in the SEM images (see Fig. 2b). Thus, the microspheres have many active positions on the surface and possess large surface areas, which may make them suitable for potential application in the field of catalysis [26].

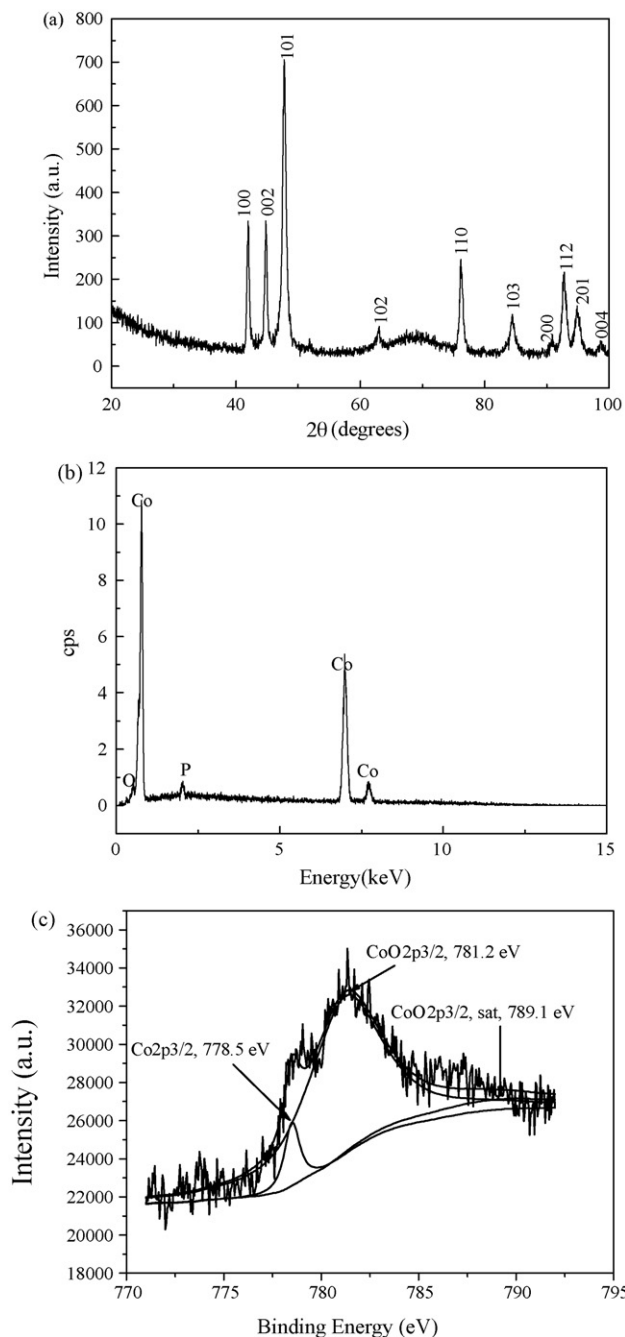


Fig. 1. (a) XRD pattern, (b) EDS pattern and (c) XPS spectrum (at a depth of 0 nm) of a sample prepared at 100 °C.

The concentration of the surfactant is crucial for the formation of the Co microspheres. In the absence of surfactant and with other parameters unchanged, only irregular crystals are formed (see Fig. 3a). In addition, with unchanged 2 mmol  $\text{CoCl}_2$ , it is found that the starting molar ratio of  $\text{SDS}/\text{Co}^{2+}$  in the solution has a large effect on the morphology of the cobalt microspheres. When this ratio is smaller than 1/3 or larger than 3, only part of prepared products are of spherical shapes. The same phenomenon is found when SDS is replaced by CTAB. Self-assembled chains consisting of relatively uniform cobalt microspheres can be obtained by adjusting the  $\text{CTAB}/\text{Co}^{2+}$  ratio range from 1/4 to 1 (see Fig. 3b). It is generally believed that the surfactant selectively absorbs on a certain crystal facet of the as-prepared

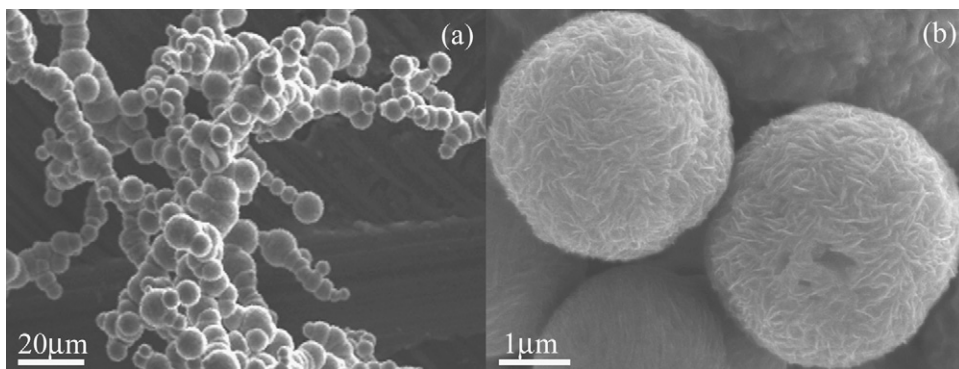


Fig. 2. SEM images of a sample obtained at 100 °C: (a) the general morphology and (b) the local morphology.

nanoparticles, resulting in the assembled structures, such as nanowires, nanobelts and nanospheres [24–25]. It has been reported that the surfactants SDS and CTAB can be used to obtain a special structure in the hydrothermal synthesis [30–32]. In our experiments, the surfactant possibly acts as a soft template. It is believed that the formation of the nanosheets is a typical Ostwald ripening process. Initially, many nanoparticles with different sizes appear in the solution. With the reaction proceeding, the nanoparticles with larger size grow at the cost of the smaller ones due to their higher surface free energy [33]. Li et al. reported a similar result in the synthesis of nanostructures [34]. In the subsequent process, the Co particles diffused, aggregated together and thus assembled into cobalt nanosheets due to their natural properties and the assistance of the surfactant. Finally, both the individual nanosheets assembled into the spheres and then the spheres assembled into cobalt chains can be ascribed to the magnetic dipole–dipole interaction and the effects of the surfactant [35].

To investigate the influence of sodium tartrate ( $\text{Na}_2\text{C}_4\text{H}_4\text{O}_6$ ) on the morphology of the cobalt microspheres, the same molar of sodium citrate ( $\text{Na}_3\text{C}_6\text{H}_5\text{O}_7$ ) was used to replace the sodium tartrate, while other experimental conditions were kept the same. As shown in Fig. 4a, the result indicates that only hexagonal-cobalt sheets are obtained. It is found that a dendritic structure instead of the Co microspheres form at a low starting molar ratio of  $\text{Na}_2\text{C}_4\text{H}_4\text{O}_6/\text{Co}^{2+}$  (below 10), with all other reaction conditions the same (Fig. 4b). The optimal starting molar ratio of  $\text{Na}_2\text{C}_4\text{H}_4\text{O}_6/\text{Co}^{2+}$  for fabricating chains of cobalt microspheres ranges from 15 to 20. However, when we optimized the starting ratio of  $\text{Na}_3\text{C}_6\text{H}_5\text{O}_7/\text{Co}^{2+}$ , only mono-dispersed cobalt microspheres without chains were observed (Fig. 5a and b). The proper ratio of  $\text{Na}_3\text{C}_6\text{H}_5\text{O}_7/\text{Co}^{2+}$  for obtaining only spherical products ranges from 1 to 5. If this ratio is increased, not only microspheres, but also thin sheets and some products with irregular shapes will form. In contrast with the situation when the complex reagent  $\text{Na}_2\text{C}_4\text{H}_4\text{O}_6$  was used, the microspheres obtained did not form chain structures. This may be due to the different molecular structures of  $\text{Na}_3\text{C}_6\text{H}_5\text{O}_7$  and  $\text{Na}_2\text{C}_4\text{H}_4\text{O}_6$ . Without using sodium tartrate or

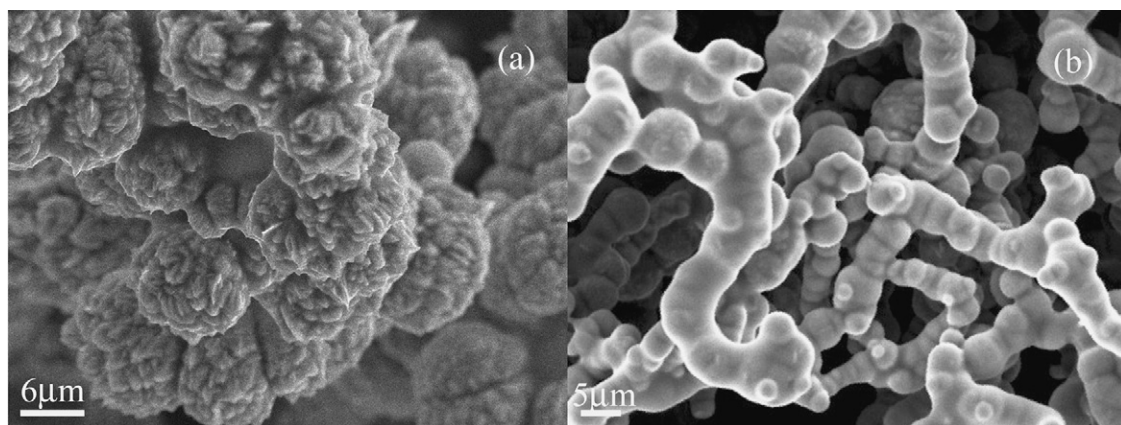


Fig. 3. SEM images of samples obtained at 100 °C: (a) in the absence of SDS and (b) in the presence of CTAB ( $\text{CTAB}/\text{Co}^{2+} = 1/4$ ).

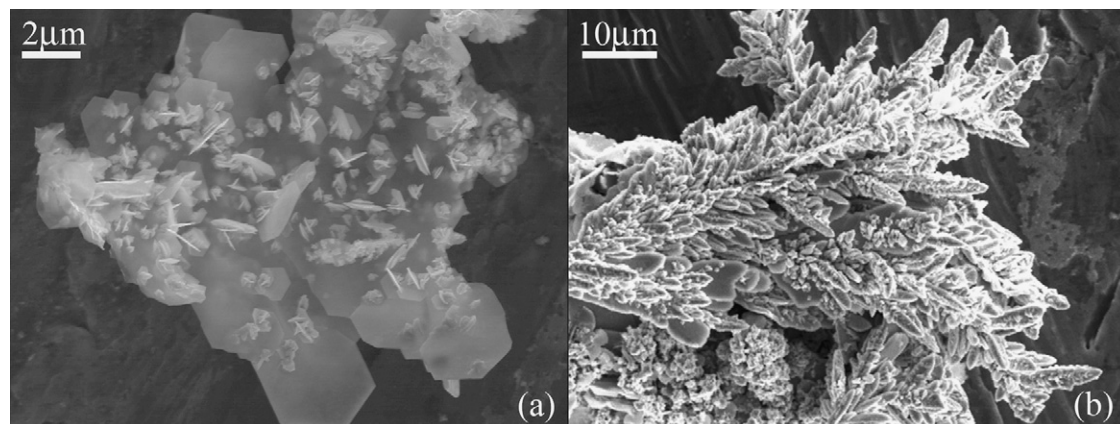


Fig. 4. SEM images of samples obtained at 100 °C: (a) with the complex reagent sodium citrate and (b) at the starting molar ratio  $\text{Na}_2\text{C}_4\text{H}_4\text{O}_6/\text{Co}^{2+} = 10$ .

sodium citrate, the sample mainly consisted of cobalt oxide. The complexes  $\text{Co}(\text{C}_4\text{H}_2\text{O}_6)^{2-}$  and  $[\text{Co}(\text{C}_6\text{H}_5\text{O}_7)^2]^{4-}$  form if the complex reagents  $\text{Na}_2\text{C}_4\text{H}_4\text{O}_6$  and  $\text{Na}_3\text{C}_6\text{H}_5\text{O}_7$  are respectively used. Therefore, the concentration of free cobalt ions in the solution sharply decreases, resulting in a low reaction rate. This low reaction rate may be favorable for the formation of the cobalt microspheres. In addition, the formation of the complexes  $\text{Co}(\text{C}_4\text{H}_2\text{O}_6)^{2-}$  or  $[\text{Co}(\text{C}_6\text{H}_5\text{O}_7)^2]^{4-}$  avoids the generation of cobalt hydroxide, which avoids the formation of cobalt oxide.

During the experimental processes, it was found that both the reaction temperature and the alkalinity contribute to the reaction rate, which leads to the formation of the different cobalt morphologies. When the reaction proceeded at 50 °C, the solution was still dark purple and only a small amount grey precipitation was found at the bottom of the autoclave after 48 h, which indicates that the reaction had not completely finished. However, the reaction can be completely finished within 10 h at 80 °C. Although the products at lower temperatures (50–90 °C) are chain-like cobalt, the individual spheres are non-uniform and their surface morphologies are different. For instance, as seen from Fig. 6a–c, when the reaction was carried out at 80 °C, there are two kinds of spheres. One kind is a flower-like sphere composed of a lot of nanosheets, which is similar to that in Fig. 2 (see Fig. 6b); the other kind is a sphere constructed compact-stacked nanosheets (see Fig. 6c). The reaction rate increases with increasing the reaction temperature. When the reaction temperature was increased to 150 °C, square-like crystals were observed, as shown in Fig. 6d. The optimal temperature for the formation of the cobalt microspheres was determined to be between 100 °C and 140 °C. The redox reaction during the hydrothermal treatment was under alkaline condition and, therefore, the alkalinity influenced the kinetics of the reaction. In a certain concentration range (0.5–5 M), variation of the NaOH concentration in the

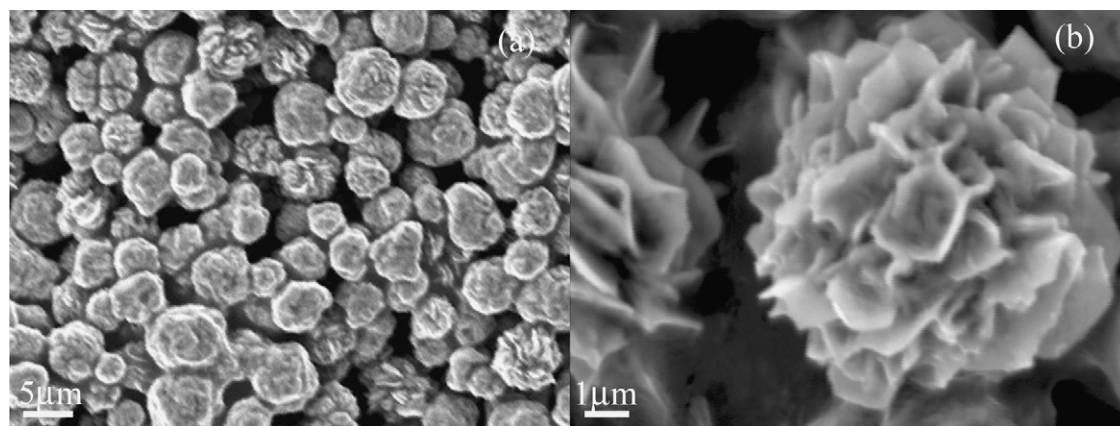


Fig. 5. SEM images of samples obtained at 100 °C with  $\text{Na}_3\text{C}_6\text{H}_5\text{O}_7$  and SDS ( $\text{Na}_3\text{C}_6\text{H}_5\text{O}_7/\text{Co}^{2+} = 1$ ): (a) the general morphology and (b) the local morphology.

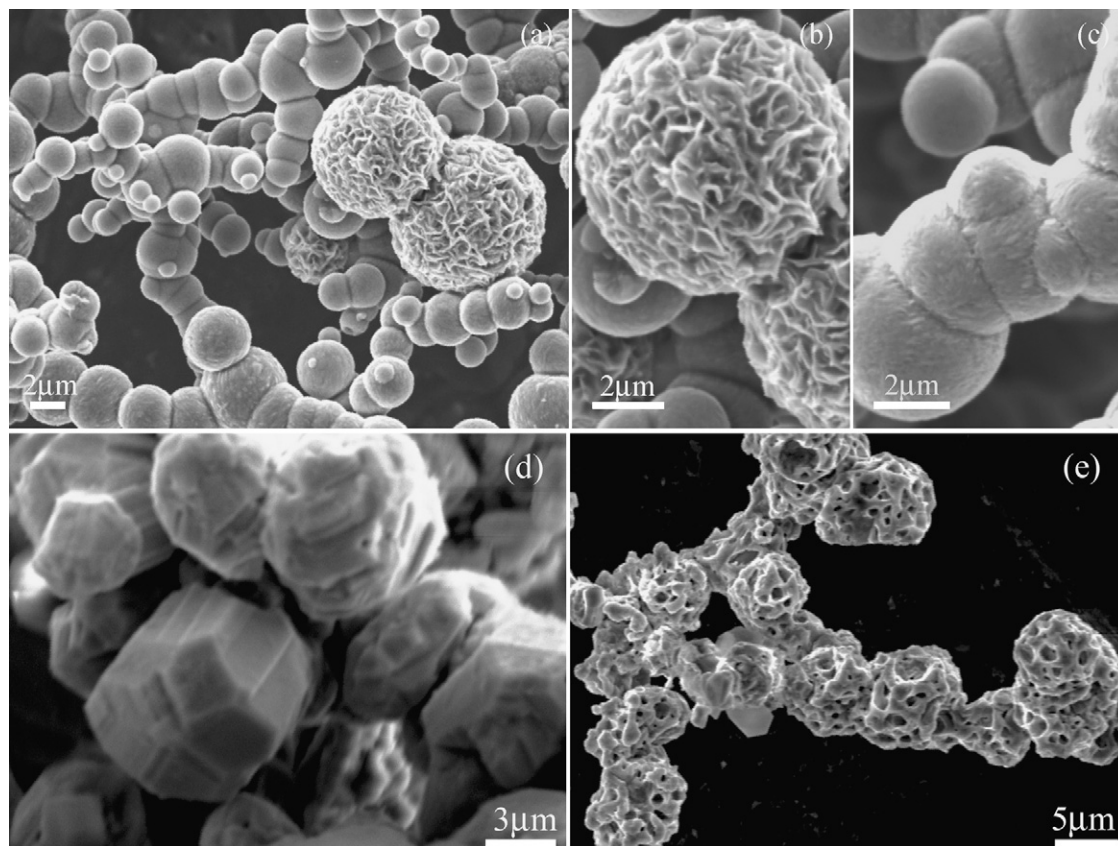


Fig. 6. SEM images of samples obtained (a–c) at a reaction temperature of 80 °C, (d) at a reaction temperature of 150 °C, (e) at 100 °C and naturally cooled in air.

solution only changed the reaction rate: the higher the NaOH concentration the faster the reaction. When the starting solution NaOH was 1 M, the redox reaction could not complete even after 20 h but, with a concentration of 5 M NaOH, the reaction could finish after a hydrothermal treatment for 8 h. For the formation of cobalt microspheres, the optimal NaOH concentration ranges from 2 M to 5 M. Further increasing the concentration of NaOH in the solution, we obtained the products with irregular morphologies, which may be explained by variation of growth rates. When the concentration of NaOH is raised, the growth rate is accelerated, which is likely unfavorable for the formation of spherical structures. Under typical experimental conditions, it was found that, when the autoclaves were naturally cooled in the air instead of rapidly cooled by water, some porous spheres were present (see Fig. 6e, estimated to be about 5% by SEM). The mechanism for the formation of the porous cobalt spheres is not clear, and a further study is under way.

The magnetic hysteresis loops of the cobalt chains obtained after hydrothermal treatment at 100 °C for 10 h were measured at 5 K and 300 K. The hysteresis loops were recorded at each temperature, after a magnetic field of 20 kOe was applied. It can be seen in Fig. 7 that the values of the coercivity field ( $H_c$ ) at 5 K and 300 K are 235 Oe and 146 Oe, respectively. The coercivity at room temperature is much higher than that of bulk cobalt (a few tens of oersteds [36]), which may be attributed partially to the shape anisotropy of the nanosheets composing the cobalt microspheres and partially to the chain structure. However, the coercivity of the chains is much lower than that of 1D Co nanowires (166.8 Oe, 300 K) [24] and of nanobelts (410.6 Oe, 300 K) [25]. There are several possible explanations for this reduction of the coercivity. It may be attributed to surface oxidation because the sample is inevitably exposed to air; another possibility may be due to remaining surfactant that cannot be completely washed out. In addition, the 3D spherical structure has smaller shape anisotropy than 1D nanomaterials [24–25]. The coercivities of the Co samples with dendritic (Fig. 4b) and hexagonal sheet shapes (Fig. 4a) at 5 K are 223 Oe and 237 Oe, respectively. Their coercivities decrease with increasing temperature, which are reduced to 123 Oe and 158 Oe at 300 K, respectively. The

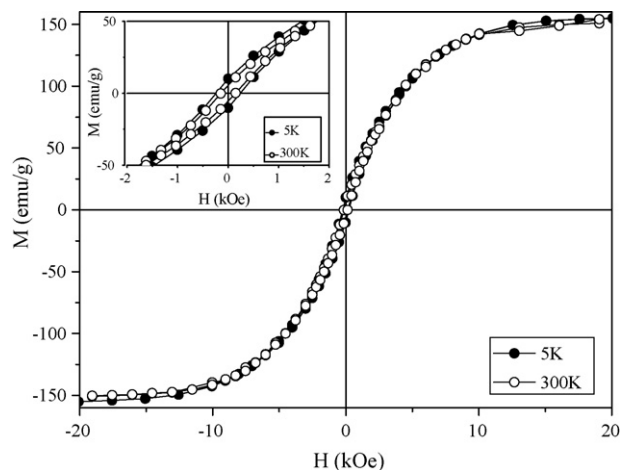


Fig. 7. Magnetic hysteresis loops at 5 K (filled circles) and 300 K (open circles) of cobalt chains. The inset shows the low-field part of the hysteresis loops.

coercivity of the hexagonal cobalt sheet is slightly higher than that of the cobalt spheres, which is possibly due to the difference in the shape anisotropy. At 300 K, the saturation magnetization  $M_s$  is  $150.6 \text{ emu g}^{-1}$  which is slightly smaller than the bulk value ( $168 \text{ emu g}^{-1}$  [24]). It has been reported that surface oxidation at the grain boundaries causes the decrease of the  $M_s$  [34]. In our experiments, surface oxidation may be one reason for the decrease of the  $M_s$  [24]; another reason may be the existence of a very small amount of complex reagents and surfactant in the product, although the product has been washed several times before measurement [37–38].

Zero-field-cooled (ZFC) and field-cooled (FC) magnetization curves of the microspheres are shown in Fig. 8. The bifurcation between the ZFC and FC curves indicates irreversible magnetic behavior. However, the absence of the peak in the ZFC curve suggests that the blocking temperature  $T_B$  is far above room temperature. A very wide energy-barrier distribution can be deduced from the continuous increase of magnetization in the ZFC curve [39]. Therefore, the ZFC magnetization can be ascribed mainly to domain-wall depinning in multidomain microspheres, similar to the case of nanocapsules [22,39]. The change in the FC magnetization at about 150 K suggests that there might be an antiferromagnetic phase in the cobalt spheres. This is possibly due to the formation of cobalt oxide (CoO) at the surface of the microspheres (The existence of CoO has been confirmed by the EDS and XPS patterns).

It is interesting to note that, whereas in Fig. 7 the magnetization at 50 Oe decreases with temperature, which is a normal behavior for a ferromagnet, the FC magnetization at the same magnetic field in Fig. 8 shows opposite behavior,

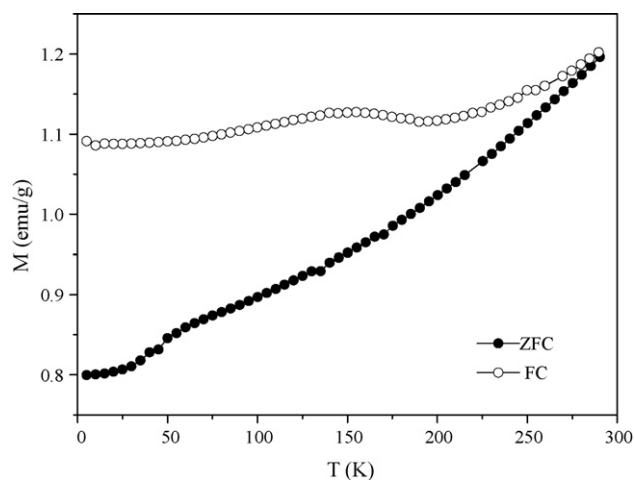


Fig. 8. Zero-field-cooled (filled circles) and field-cooled (open circles) magnetization curves of cobalt chains.

i.e. increases with temperature. At the first glance, the results in Figs 7 and 8 are somewhat contradictory. This FC behavior seems to be inconsistent with previous work on other nanocapsules, like FeCo(C) [21] and Fe(B) nanocapsules [39]. This unusual behavior can be understood as follows: the increase of the FC magnetization with increasing temperature may be attributed to the relatively low applied field of 50 Oe and increased thermal activity is still needed to overcome the comparatively high anisotropy energy barriers to align the magnetic moments along the direction of the field. According to the relation  $25k_B T_B = KV$  [39], the large anisotropy constant of Co (compared to Fe) and the large volume  $V$  of the microspheres may result in a high blocking temperature  $T_B$ . Therefore, the anisotropy energy barriers  $KV$  in the present microspheres are much higher than in the FeCo(C) [22] and Fe(B) [39] nanocapsules. It is understandable that to observe the FC behavior as for FeCo(C) [22] and Fe(B) [39], a comparatively high field should be applied, higher than those applied in the cases of FeCo(C) [22] and Fe(B) [39].

#### 4. Conclusions

In summary, a hydrothermal reduction process is reported for the synthesis of self-assembled cobalt chains of microspheres which consist of nanosheets. A surfactant and a complex reagent were used to control the morphologies of the cobalt nanostructures. The reaction conditions, including the reaction temperature, the starting molar ratio of SDS/Co<sup>2+</sup> (CTAB/Co<sup>2+</sup>), Na<sub>2</sub>C<sub>4</sub>H<sub>4</sub>O<sub>6</sub>/Co<sup>2+</sup> (Na<sub>3</sub>C<sub>6</sub>H<sub>5</sub>O<sub>7</sub>/Co<sup>2+</sup>) and the alkalinity of the solution, were found to be the key parameters for the formation of cobalt microspheres. The chains exhibit ferromagnetic behavior. It can be expected that, based on this synthesis method which is very important for controlled inorganic synthesis, many other kinds of applicable magnetic materials and self-assembled magnetic devices with various structures may be developed.

#### Acknowledgement

This work has been supported by the National Nature Science Foundation of China under project no. 50331030.

#### References

- [1] J. Chen, D.H. Bradlurst, S.X. Dou, H.K. Liu, *J. Electrochem. Soc.* 146 (1999) 3606.
- [2] S.H. Sun, *Adv. Mater.* 18 (2006) 393.
- [3] C.B. Murray, C.R. Kagan, M.G. Bawendi, *Science* 270 (1995) 1335.
- [4] A.P. Alivisatos, *Science* 271 (1996) 933.
- [5] D. Weller, M.E. Doerner, *Annu. Rev. Mater. Sci.* 30 (2000) 611.
- [6] Y.P. Bao, M. Beerman, K.M. Krishnan, *J. Magn. Magn. Mater.* 266 (2003) L245.
- [7] S.A. Davis, M. Breulmann, K.H. Rhodes, B. Zhang, S. Mann, *Chem. Mater.* 13 (2001) 3218.
- [8] M.D. Lynch, D.L. Patrick, *Nano Lett.* 2 (2002) 1197.
- [9] K.M. Ryan, D. Ertz, H. Olin, M.A. Morris, J.D. Holmes, *J. Am. Chem. Soc.* 125 (2003) 6284.
- [10] M.S. Wong, J.N. Cha, K.S. Choi, T.J. Deming, G.D. Stucky, *Nano Lett.* 2 (2002) 583.
- [11] S.D. Hersee, X.Y. Sun, X. Wang, *Nano Lett.* 6 (2006) 1808.
- [12] D.P. Dinépa, M.G. Bawendi, *Angew. Chem. Int. Ed.* 38 (1999) 1788.
- [13] H. Yoshikawa, K. Hayashida, Y. Kozuka, A. Horiguchi, K. Awaga, S. Bandow, S. Iijima, *Appl. Phys. Lett.* 85 (2004) 5287.
- [14] C.P. Graf, R. Birringer, A. Michels, *Phys. Rev. B* 73 (2006) 212401.
- [15] H.Q. Cao, Z. Xu, H. Sang, D. Sheng, C.Y. Tie, *Adv. Mater.* 13 (2001) 121.
- [16] J.L. Legrand, A.T. Ngo, C. Petit, M.P. Pileni, *Adv. Mater.* 13 (2001) 58.
- [17] G.M. Whitesides, B. Grzybowski, *Science* 295 (2002) 2418.
- [18] P. Yang, *Nature* 425 (2003) 243.
- [19] H.L. Niu, Q.W. Chen, H.F. Zhu, Y.S. Lin, X. Zhang, *J. Mater. Chem.* 13 (2003) 1803.
- [20] X.L. Dong, Z.D. Zhang, Y.C. Chuang, S.R. Jin, *Phys. Rev. B* 60 (1999) 3017.
- [21] X.L. Dong, Z.D. Zhang, S.R. Jin, B.H. Kim, *J. Appl. Phys.* 86 (1999) 6701.
- [22] Z.D. Zhang, J.G. Zheng, I. Škorpánek, G.H. Wen, J. Kováč, F.W. Wang, J.L. Yu, Z.J. Li, X.L. Dong, S.R. Jin, W. Liu, X.X. Zhang, *J. Phys. Cond. Matt.* 13 (2001) 1921.
- [23] Z.D. Zhang, *J. Mater. Sci. Technol.* 23 (2007) 1.
- [24] Q. Xie, Y.T. Qian, S.Y. Zhang, S.Q. Fu, W.C. Yu, *Eur. J. Inorg. Chem.* (2006) 2454.
- [25] Q. Xie, Z. Dai, W.W. Huang, J.B. Liang, C.L. Jiang, Y.T. Qian, *Nanotechnology* 16 (2005) 2958.
- [26] Y.L. Hou, H. Kondoh, T. Ohta, *Chem. Mater.* 17 (2005) 3994.
- [27] Z.Y. Thang, N.A. Kotov, *Adv. Mater.* 17 (2005) 951.

- [28] B.J. Tan, K.J. Klabunde, P.M.A. Sherwood, *J. Am. Chem. Soc.* 113 (1991) 855.
- [29] A.B. Mandale, S. Badrinarayanan, S.K. Date, A.P.B. Sinha, *J. Electron Spectrosc. Relat. Phenom.* 33 (1984) 61.
- [30] Q. Liu, H.J. Liu, M. Han, J.M. Zhu, Y.Y. Liang, Z. Xu, Y. Song, *Adv. Mater.* 17 (2005) 1995.
- [31] X.M. Sun, Y.D. Li, *J. Coll. Inter. Sci.* 291 (2005) 7.
- [32] J. Yang, C.K. Lin, Z.L. Wang, J. Lin, *Inorg. Chem.* 45 (2006) 8973.
- [33] Z.P. Liu, Y. Yang, J.B. Liang, Z.K. Hu, S. Li, S. Peng, Y.T. Qian, *J. Phys. Chem. B.* 107 (2003) 12658.
- [34] Y.Y. Li, J.P. Li, X.T. Huang, G.Y. Li, *Cryst. Growth Des.* 7 (2007) 1350.
- [35] J.H. Gao, B. Zhang, X.X. Zhang, B. Xu, *Angew. Chem. Int. Ed.* 45 (2006) 1220.
- [36] H.Q. Cao, Z. Xu, H. Sang, D. Sheng, C.Y. Tie, *Adv. Mater.* 13 (2006) 121.
- [37] G. Dumpich, T.P. Krome, B. Hausmanns, *J. Magn. Mater.* 248 (2002) 241.
- [38] B. Hausmanns, T.P. Krome, G. Dumpich, *J. Appl. Phys.* 93 (2003) 8095.
- [39] Z.D. Zhang, J.L. Yu, J.G. Zheng, I. Skorvanck, J. Kovac, X.L. Dong, Z.J. Li, S.R. Jin, H.C. Yang, Z.J. Guo, W. Liu, X.G. Zhao, *Phys. Rev. B* 64 (2001) 024404.